A Nonlinear Adaptive Equalization Technique in Digital Communication II

Qadeer Ul. Hasan
Department of Electronics and Communications Engineering,
American University of Ras Al Khaimah
Ras Al Khaimah, UAE
qhasan@aurak.ae, drqadeer.hasan@gmail.com

Rafiqul Zaman Khan
Department of Computer Science, Aligarh Muslim University, Aligarh, India
rzkhan.cs@mail.amu.ac.in , rzk32@yahoo.co.in

Lev B. Levitin
Department of Electrical and Computer Engineering, Boston University
Boston, Massachusetts, USA
evitin@bu.edu

ABSTRACT: *An approach to rectify the distortions caused by the Travelling Wave Tube (TWT) or solid-state High Power Amplifiers (HPA) used in digital satellite communication systems and at the same time to correct the effects of intersymbol interference is presented. Linear adaptive signal processing techniques fail to eliminate these nonlinear distortions introduced by nonlinear components in the satellite channel. Here we present a nonlinear adaptive signal processing technique based on Volterra series. First part of this paper [15] includes mathematical description of proposed scheme. This part includes computer simulation and results obtained.*

Key Words: QPSK, QAM, TWT, HPA

Received: 1 October 2009, Revised 14 November 2009, Accepted 19 November 2009

1. Introduction

Adaptive signal processing techniques have been used in many diverse fields [1, 6] and found to be quite effective. Many of these techniques were developed for linear systems and are linear in nature. In part I of this paper [15], we provided mathematical details about a nonlinear technique to counter the adverse effects (nonlinear amplitude and phase distortion) caused by high power amplifiers (HPA) in addition to inter symbol interference present in the satellite communication channels.. The HPA are usually based on either traveling wave tube (TWT) or solid-state GaAs FET and have nonlinear input/output characteristics [8].

Our technique takes advantage of the fact that Volterra series can be used to model the various types of nonlinearities. Volterra series is also suitable to model the linear-memoryless nonlinear and linear (LNL) types of nonlinearities present in the digital communication systems [2, 3, 4, 5, 9, 10, 12, 13]. Digital satellite communication channel in our study is also LNL type and we propose a technique based on Volterra series model to counter the adverse affects of HPA in addition to mitigating the affects of ISI. We design a nonlinear adaptive equalizer based on this technique to recover the originally transmitted data. Adaptive equalizer design usually belongs to two groups; data-aided and blind zero forcing. We follow the data-aided scheme to train our nonlinear equalizer. Once trained, we assume that nonlinearity in HPA (due to aging of amplifier) and example for mobile phones) since it wastes valuable resource (bandwidth). However, in satellite communication, channel characteristics changes significantly, a known training sequence is used to adapt the nonlinear equalizer.

We, also, assume that signal to noise ratio (S/N) is very high in the uplink segment of the channel, therefore we can safely ignore affects of noise in uplink segment simulations.

2. Volterra Series Based Adaptive Signal Processing

Noise and Inter Symbol Interference (ISI) are two main factors that adversely affect the performance of the digital communication systems. In order to combat these effects, various channel equalization techniques have been developed. These techniques are able to counter the ISI present in the channel and enabling the communication channel to increase its throughput and reduce the probability of error. A major building block in these adaptive equalizers is the adaptive linear combiner or transversal filter. While the linear equalizations have been found to be quite effective for equalizations of channels with small to moderate amplitude distortions, they fail when the amplitude modulation is severe. This usually happens in multi-path propagations. In those cases, decision feedback equalizers (DFE) have been found more effective [11]. Also, linear equalization techniques that work in the case of ISI produced by linear channel fail to work if a nonlinear element is introduced in the channel. To overcome this problem we propose a nonlinear adaptive filter based on the Volterra series. Linear adaptive filter is a subset of this filter. We use LMS algorithm with our non-linear adaptive filter because of its simplicity. (Details of this algorithm can be found in [7, 14]). This algorithm can be explained in three steps:

1. Filter output: $$y[n] = \sum_{k=0}^{M-1} w_k x(n-k) \quad (2.1)$$

here the weights are multiplied with the tap-inputs and the sum represents an estimate of desired output.

2. Estimation error: $$e[n] = d[n] - y[n] \quad (2.2)$$

3. Tap-weights adaptation: $$w[n+1] = w[n] + \mu e[n] x[n] \quad (2.3)$$

It should be noted that the second term in equation (2.3) represents the correction that is applied to current estimate of the tap-weights, as the error goes down, which means that when our estimate of desired output is approaching the desired output, the correction components decrease and the weights start to converge to the final value.
3rd order Volterra with finite memory M is reproduced here.

$$y_n = \sum_{i=0}^{M} w_i x_{n-i} + \sum_{i=0}^{M}\sum_{j=0}^{M} w_{ij} x_{n-i} x_{n-j} + \sum_{i=0}^{M}\sum_{j=0}^{M}\sum_{k=0}^{M} w_{ijk} x_{n-i} x_{n-j} x_{n-k} \quad (2.4)$$

M is number of taps we use in our transversal filter. x_{n_*} are the inputs entered in the system one at a time. $x_{n-i}x_{n-j}$ and $x_{n-i}x_{n-j}x_{n-k}$ are quadratic and cubic terms generated from the inputs x_{n_*}, and w_*, are the transversal filter weights that are updated in each iteration. We use the symmetry property to keep the number of terms to a minimum in the transversal filter.

3. Operation of Non-Linear Equalizer

We used our nonlinear filter with QAM modulation scheme. QAM is known to have variable amplitude signal and pose a real challenge to recover it after passing through nonlinearity. The operation of the modified QAM equalizer [11] is described

Number of Taps	1	2	3	4	5	6
Linear Terms	1	2	3	4	5	6
Quadratic Terms	1	2	5	9	14	20
Cubic Terms	1	4	10	20	35	56

Table 1. Number of Terms of Transversal Filter

below. The outputs from the demodulator are fed to the QAM equalizer shown in Fig. 14 [11]. This equalizer is actually consists of four separate equalizer but with two sets of weights only. Each equalizer makes a prediction, and then these predictions are combined to form the final in-phase and in-quadrature channel prediction or estimate of the desired output. Both in-phase and in-quadrature channels produce errors, these errors are then used to update both sets of weights and the process starts all over again. Once the training sequence is over and the filter weights have been converged, we start the actual data through the system. The only difference this time around is that we make decisions based on the predicted in-phase and in-quadrature channel and use these as reference to generate the set of errors that in turn updates the weights. This is a continuous process that is time-consuming, but it keeps track of small changes in the system over the period of time. The mathematical description of the above QAM equalizers is as follows:

$$pred_{in}1 = \sum_{k=0}^{M-1} w_{in}(k)x_{in}(n-k), \text{ and } pred_{in}2 = \sum_{k=0}^{M-1} w_{qu}(k)x_{in}(n-k)$$
$$pred_{qu}1 = \sum_{k=0}^{M-1} w_{in}(k)x_{qu}(n-k), \text{ and } pred_{qu}2 = \sum_{k=0}^{M-1} w_{qu}(k)x_{qu}(n-k) \quad (3.1)$$

The equation to predict the in-phase and quadrature channel is

$$in_{pred} = pred_{in}1\text{-}pred_{qu}2 = \text{and } qu_{pred} = pred_{in}2 + pred_{qu}1 \quad (3.2)$$

Let us define the two errors produced by these estimates.

$$e_{in} = in_{pred}\text{-}actual_{in} \text{ and } e_{qu} + qu_{pred}\text{-}actual_{qu} \quad (3.3)$$

These errors are then used to update the two sets of weights and the expression for that is shown below:

$$w_{in}[n+1\} = w_{in}[n] - 2(\mu e_{in}[n]x_{in}[n] + \mu e_{qu}[n]x_{qu})$$
$$w_{qu}[n+1\} = w_{qu}[n] - 2(\mu e_{qu}[n]x_{in}[n] + \mu e_{in}[n]x_{qu}) \quad (3.4)$$

Once the equalizer is trained using the above procedure, the only operation different from the above is calculating the error. When the channel is trained, we take the predicted outputs of the in-phase and in-quadrature channel and, based on where they fall in the decision region, make decisions. The decided symbols are used to find out the errors to update the weights. The value of μ used in our simulations is 0.003. The values of μ usually fall between $0 < \mu < \frac{2}{\text{total input power}}$ [13], [13], where the term total input power refers to the sum of the mean square values of the tap inputs. The convergence characteristics of nonlinear equalizer are similar to that of a linear equalizer [7].

To calculate the number of symbol errors, we take the pair from in-phase and in-quadrature channel and compare it with the transmitted in-phase and in-quadrature symbols. Both predicted symbols have to match with the transmitted ones to declare that a correct estimate was made; otherwise it is a symbol error.

4. Simulations and Analysis

We performed computer simulations to validate the proposed nonlinear adaptive filter starting with the QPSK modulated signal. After that we continue with more challenging 16QAM scheme. We use Matlab to generate the random data for our simulation. We generated two sets of equiprobable sequences for the in-phase and in-quadrature channel. We used two sets of twelve million data points for our simulation for the in-phase and in-quadrature channels for QPSK modulation and 40 million data points for 16-QAM modulation. We used 2,000 data points to train the equalizer. Monte Carlo type of simulation used to find out the number of symbol errors. Since we assume a gray coding, the symbol error rate is equal to bit error rate. It was observed that the equalizer was trained with fewer than 1,000 data points in both cases.

4.1 QPSK Simulations and Results

We start with a scatter diagram of QPSK (Fig. 2L). This diagram will serve as a reference when we show the effects of a linear filter and nonlinearity on a QPSK signal. In Fig. 2R, we show the scatter plot for QPSK for the case where the signal has

passed through the linear filter, we are assuming the ISI with limited memory, and in this particular case it goes to only two previous pulses. In Fig. 3L, we have the scatter plot for the signal, after it has passed through the nonlinearity. We apply nonlinear equalization to the signal that has passed through the linear filter and through the nonlinearity, without adding any noise to it. The result of this equalization is shown in Fig. 3R. We can see that the signal points are brought back to the original locations or very close to original locations.

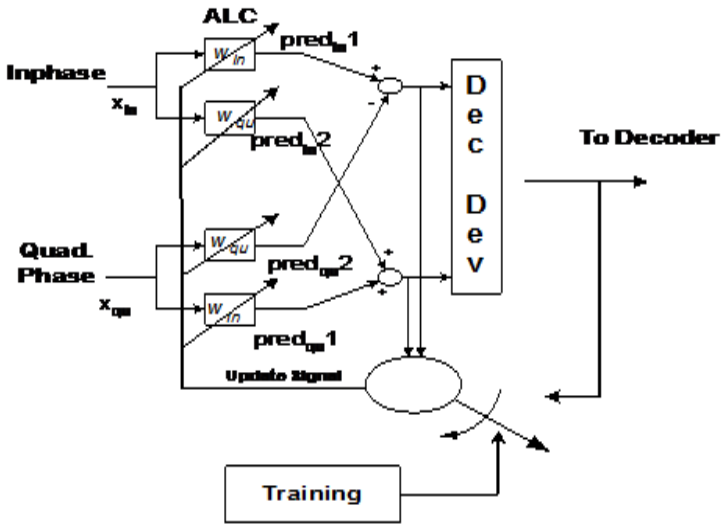

Figure 1. QAM Equalizer

We experimented with three different level of ISI (blue with least and Red with most) in our simulations and it is shown in Fig. 4 for before and after the nonlinearity case. From our simulation we found that there was practically no difference between the performance of the linear adaptive equalizer and the nonlinear equalizer and this result was expected because the effects of the nonlinearity are not very severe in the case of constant amplitude scheme such as QPSK. The increase in ISI interference levels however did make a difference as will be evident from our results in Table 3. Next we will show two scatter plots of QPSK with noise before and after the equalization. This can be seen in Fig. 5. In Fig 6, prediction error is shown and it goes down very quickly while non-linear equalizer (NLE) is being trained using the training sequence.

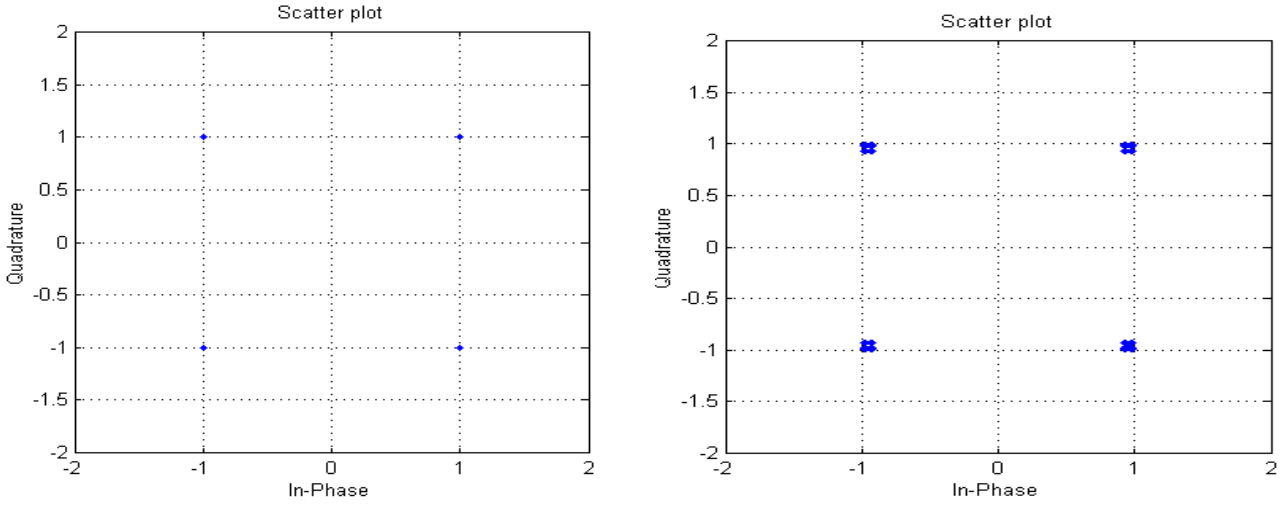

Figure 2. QPSK Scatter Plot: Reference and linear filter output for t0/T= 0.150.15

In the next table, we will present the symbol error rate in the presence of noise, we will only present the result for nonlinear equalizer since there is virtually no difference in performance between linear and nonlinear equalizer. The number of symbol errors are 6 per 12x106, when ratio of t0/T= 0.15.

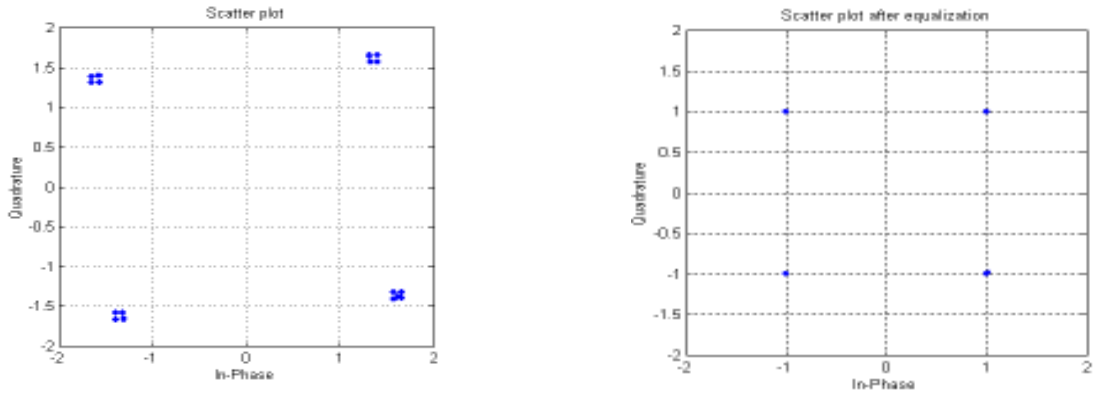

Figure 3. QPSK Scatter Plot: Signal at the Output of Nonlinearity and after equalization

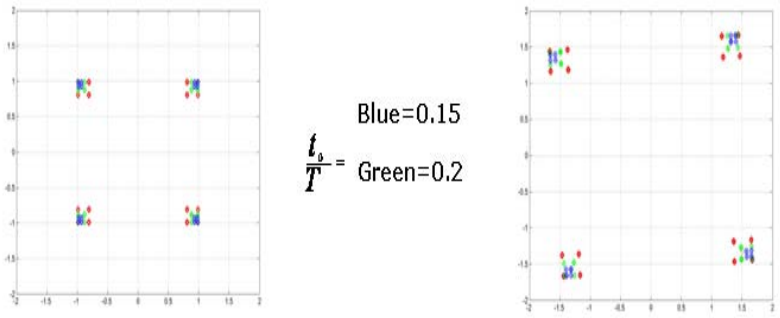

Figure 4. QPSK Scatter Plots: Effects of Different Level of ISI at the Output of Linear Filter and ISI plus Nonlinearity at the Output of nonlinear Device

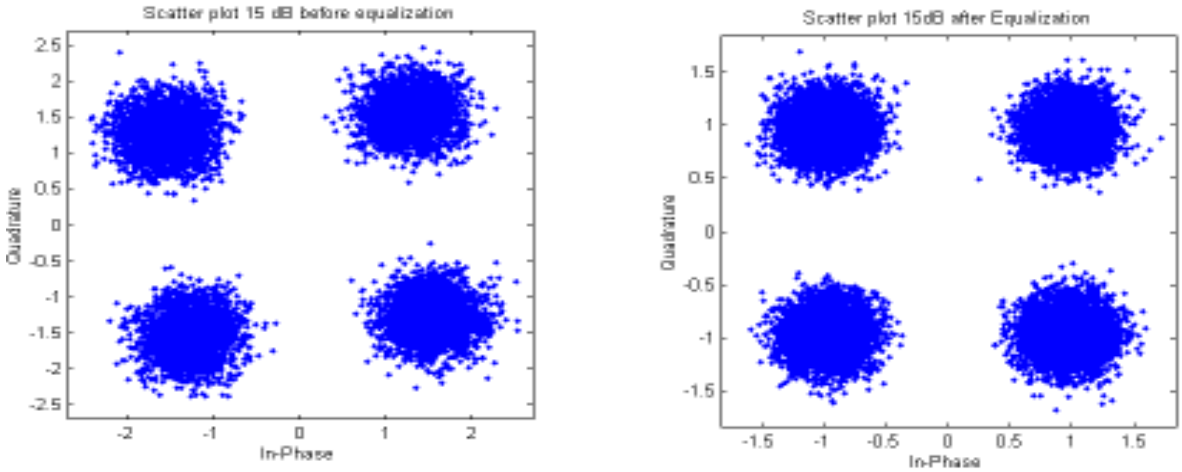

Figure 5. QPSK Scatter Plot: Signal with Noise after Nonlinearity and Equalized Signal with Noise

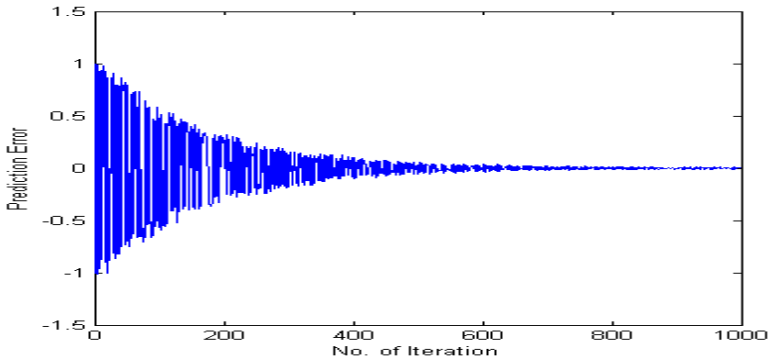

Figure 6. Error Convergence

We will estimate the standard deviation for this symbol error rate. The probability of symbol error is equal to 0.5x10-6. The standard deviation can be found using:

$$\sigma = \sqrt{\rho(1-\rho)N} \qquad (4.1)$$

where ρ is the symbol error probability and N is the total number of symbol used in simulation. Since is very small, (1-) is equal to 1. The equation 4.1 becomes $\hat{\sigma} = \sqrt{\rho N}$ and it is equal to 2.44 per 12x106 or 0.2x10-6. Our margin of error is one standard deviation.

S/N 14dB	t0=0.15T	t0=0.2T	t0=0.25T
Symbol Error Rate	$(0.5+0.2)10^{-6}$	$(0.75+0.25)10^{-6}$	$(0.91+0.27)10^{-6}$
Errors per 12x106	6	9	11

Table 2. Symbol Error Rate for QPSK

4.2. QAM Simulations and Results

Fig. 7 (L&R) shows the scatter diagram for 16-QAM before and after the linear filter, where as Fig 8 (L&R) shows the signal at the output of the nonlinearity and signal after the nonlinear equalization. We assume that ISI interference has limited memory, and in this particular case it goes to only two previous pulses. We can see from this scatter plot the effects of ISI and nonlinear device on the signal. We can see that signal points are brought back to their original location or very close to original locations except for the signals at the corners of the constellation. To see the effects of different level of ISI, we experimented with three different level of ISI (blue with least and Red with most) in our simulations and it is shown in Fig. 9 (L&R) for before and after the nonlinearity case. From our simulation we found that linear equalizer fails to work in the case when both ISI and nonlinearity are present in the system. The nonlinear equalizer works as can be seen in the Fig 9 (L&R) and as can be seen from the results in Table 5. The increase in ISI interference did make a difference, and the number of symbol errors goes up with increase in ISI levels even though if the nonlinearity stays the same. This can be seen in Table 5. Fig 11 shows the signal with noise before and after nonlinear equalization. These correspond to S/N ratio of 25 dB. In Fig. 10R, we show the error convergence behavior of our nonlinear equalizer.

In Fig 10L red represent the scatter plot of the output of nonlinear device. Since it looks like that constellation is just rotated left, we tried to rotate it back hoping that this rotation will bring the signal points back to their respective decision regions. Green represented the rotated constellation and it can be seen that the rotation alone is not able to take care of nonlinear ISI

that was caused by the linear filter and exacerbated by the nonlinear device in our channel model. Theoretically, it is possible to change the decision regions in such a way that we can detect the signal points in the rotation-corrected signal constellation. But it cannot be done easily since position of these signal points depend on ISI as well as nonlinearity, and any change in ISI and/or nonlinearity will require change in decision regions. Finding these decision regions adaptively will increase the receiver complexity. Finally, the blue represent the equalized signal constellation and shows graphically marked improvement over the rotation alone scheme.

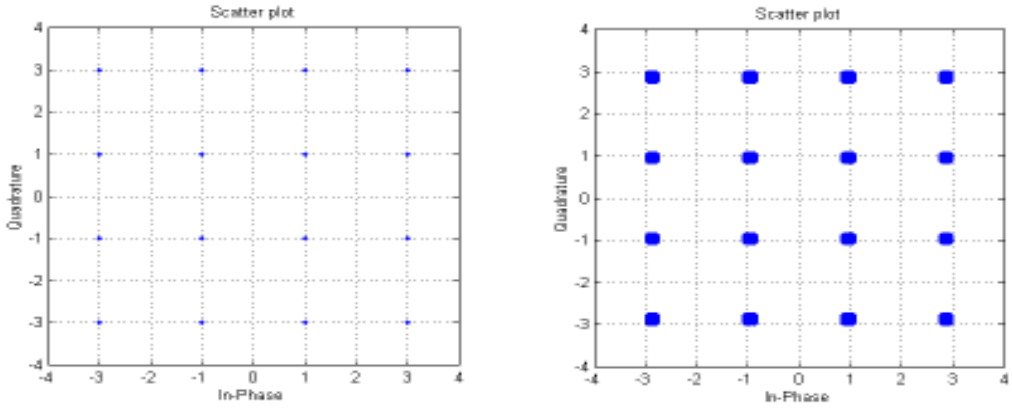

Figure 7. QAM Scatter Plot: Reference and Linear Filter Output

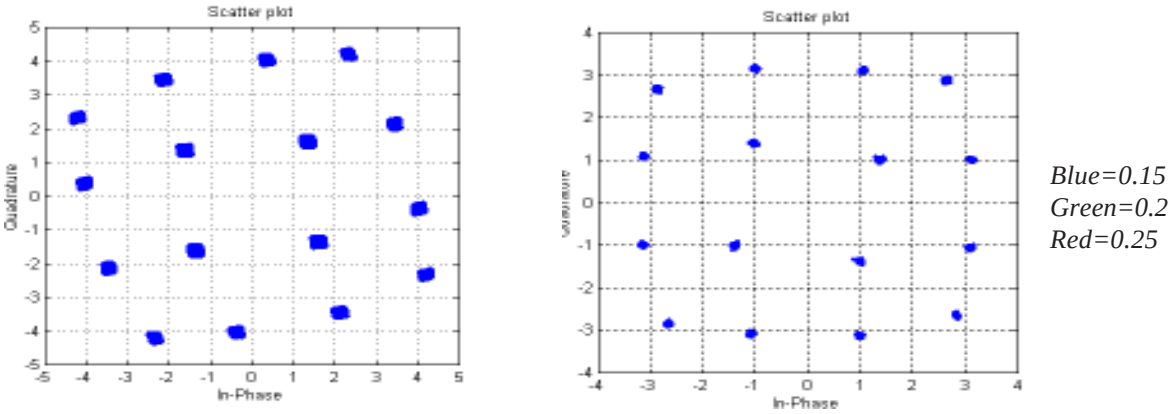

Figure 8. QAM Scatter Plot: Output of Nonlinearity and Equalized with Nonlinear Equalizer

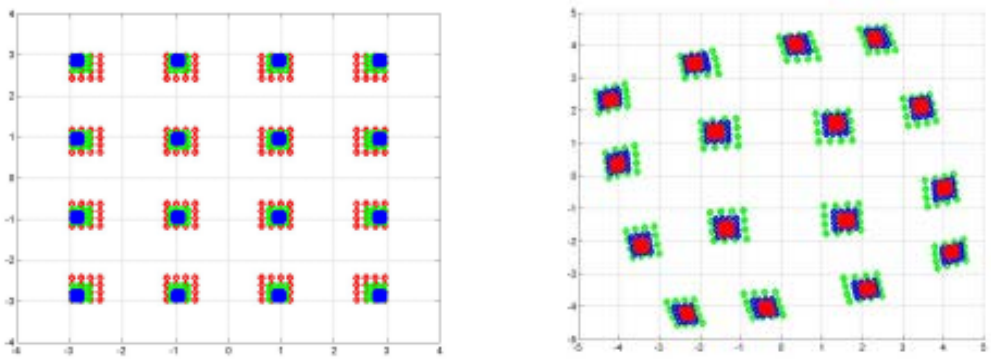

Figure 9. QAM Scatter Plot: Effects of Different Level of ISI at the Output of Linear Filter and Effects of Different Level of ISI plus Nonlinearity at the Output of Nonlinear Device for different values of t_0/T

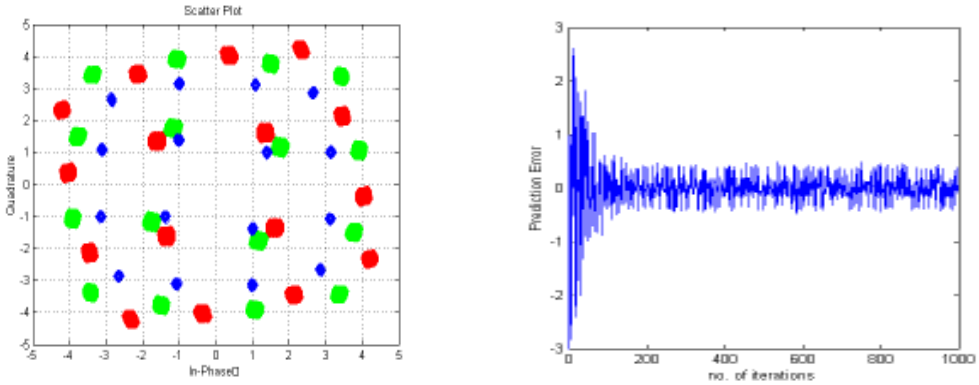

Figure 1. QAM Scatter Plot: Red is the Output of Nonlinear Device, Green Represents the Rotation only, and Blue is the Nonlinearly Equalized and Error convergence plot

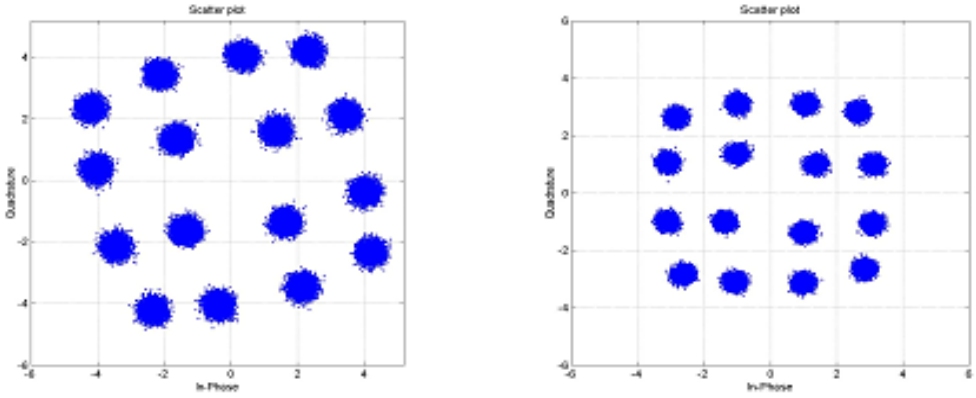

Figure 11. QAM Scatter Plot: Signal with S/N= 25 dB and Equalized Signal with S/N=25 dB

Now, we discuss the symbol error rate in the presence of noise, we will present the results for nonlinear equalizer with nonlinear element present in the channel. We will use the linear equalizer when the nonlinear element is not present in the channel. In next two tables, we will summarize the results. The number of symbol errors are 16 per 4x107, when ratio of t0/T= 0.15. The probability of symbol error is equal to 4x10-6. Number of symbols used in simulation is equal to 40x106. The standard deviation can be found using:

$$\sigma = \sqrt{\rho(1-\rho)N} \qquad (4.2)$$

where ρ is the symbol error probability and N is the total number of symbol used in simulation. Since ρ is very small, (1- ρ) is equal to 1. The equation 4.1 becomes

$$\hat{\sigma} = \sqrt{\rho N} \qquad (4.3)$$

and it is equal to 4 per 4x107 or 1x10-7. Our margin of error is one standard deviation.

S/N 22 dB	t0=0.15T	t0=0.2T	t0=0.25T
Symbol Error Rate	$(4 \pm 1)10^{-7}$	$(4.79 \pm 1.19)10^{-7}$	$(8 \pm 1.41)10^{-7}$
Errors per 4x107	14	18	23

Table 4. Symbol Error Rate for QAM with just the ISI, no nonlinear element present in the system

S/N 25dB	t0=0.15T	t0=0.2T	t0=0.25T
Symbol Error Rate	$(4 \pm 1)10^{-7}$	$(4.79 \pm 1.19)10^{-7}$	$(8 \pm 1.41)10^{-7}$
Errors per 4x107	16	23	32

Table 5. Symbol Error Rate for QAM with ISI and nonlinear element present in the system

The number of errors and probability of error for different values of S/N is presented in Table 6 and Table 7 for linear filter output (17-22 db) and nonlinearly equalized signal (19-25 db), respectively. These results are for T_0/T=0.15.

Table 6

S/N dB	No. of Errors	Probability of Error
17	1296	$(2.6x10^{-3} \pm 7.2x10^{-5})$
17.5	692	$(1.38x10^{-3} \pm 5.25x10^{-5})$
19	53	$(1.06x10^{-4} \pm 1.45x10^{-5})$
20	14	$(2.08x10^{-5} \pm 7.48x10^{-6})$
21	27 per 3.5x106	$(7.71x10^{-6} \pm 1.48x10^{-6})$
22	14 per 4x107	$(3.5 \pm 0.93x10^{-7})$

Table 7

S/N dB	No. of Errors	Probability of Error
19	1645	$(3.29x10^{-3} \pm 8.1x10^{-5})$
20	664	$(1.32x10^{-3} \pm 5.15x10^{-5})$
21	216	$(4.32x10^{-4} \pm 2.93x10^{-5})$
22	59	$(1.18x10^{-4} \pm 1.54x10^{-5})$
23	19	$(3.8x10^{-5} \pm 8.71x10^{-6})$
24	25 per 3.5x106	$(7.14 \pm 1.43x10^{-6})$
25	16 per 4x107	$(4 \pm 1x10^{-7})$

Table 6 & 7. Symbol Error and Error Probability for Linear Filter Output after Equalization (17-22 dB) and Symbol Error and Error Probability for Equalized Signal (19-25dB)

We used $0.5x10^6$ symbols for calculations in Table 6 and Table 7 except for the very last entries on both Tables where we use 4x107 symbols.

5. Conclusions

The analysis of the linear part of the communication channel shows that it is sufficient to take into account only two previous consecutive signal pulses when considering the effects of ISI in the channel. Therefore, we can limit ourselves with the memory depth M=2 in the equalization scheme. Similarly, the analysis of the effects of nonlinearity shows that it is sufficient to employ third-order Volterra filter in NLE. We used this nonlinear adaptive filter in our computer simulations. We experimented with two different kinds of modulations, QPSK (constant amplitude) and QAM (variable amplitude). We have shown that QAM, with its inherent variable amplitude, can be used in the presence of nonlinearity if we use a nonlinear equalizer.

References

[1] Adaptive Filters (1987). Special Issue, *In*: Proceedings of IEE on Communications, *Radar and Signal Processing*, 134, pt F.

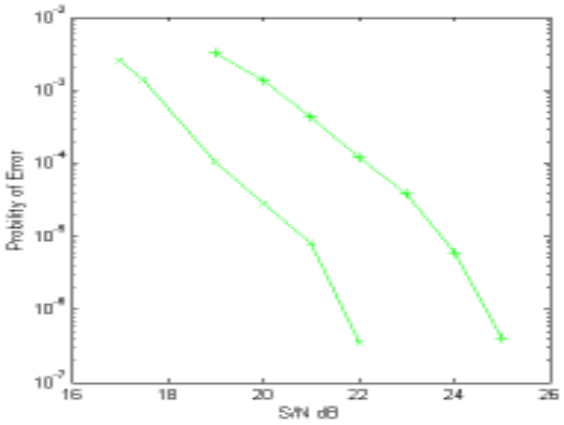

Figure 12. P(e) Plot, where x is for values in Table 6 and + is for values in Table 7

[2] Benedetto, E., Biglieri, E. (1983). Nonlinear Equalizations of Digital Satellite Channels, *IEEE Journal on Selected Areas in Communications*, SAC-1, January. 57-62.

[3] Benedetto, E., Biglieri, E., Daffara, R. (1979). Modeling and Performance Evaluation of Nonlinear Satellite Links- A Volterra Series Approach, *IEEE Journal on Aerospace and Electronics*, AES-15, 4. 494-507.

[4] De Gaudenzi, Riccardo., Loise, M. (1993). Trellis-Coded 16 QAM Transmission over a Nonlinear Satellite Channel, *In*: Proceedings of IEEE International Conference on Communication, 1723-1727.

[5] Di Benedetto, M. G., Madarini, P. (1995). A New Analog Predistortion Criterion with Application to High Efficiency Digital Radio Links, *In: IEEE Transactions on Communications*, Com-43 (12) 2966-2974.

[6] Falconer, D. D. (1978). Adaptive Equalization of Channel Nonlinearities in QAM Data Transmission Systems, *The Bell Systems Technical Journal*, 57 (7) 2589-2611

[7] Haykin, S. (1991). Adaptive Filter Theory, Prentice-Hall, Inc., Englewood Cliffs, New Jersey.

[8] Leke, A., Kenney, J. (1966). Behavioral modeling of narrowband microwave amplifiers with applications in simulating spectral re-growth, *In*: IEEE MTTs Int. Microwave Symposium Digest, 1385-1388.

[9] Lopez-Valcarce, R., Dasgupta, S. (2001). Blind Equalization of Nonlinear Channels From Second-Order Statistics", IEEE Transactions on Signal Processing, 49 (12) 3084-3097.

[10] Lopez-Valcarce, R., Dasgupta, S. (2001). Blind Equalization With Colored Sources Based on Second-Order Statistics: A Linear Prediction Approach, *IEEE Transactions on Signal Processing*, 49 (9) 2050-2059.

[11] Qurashi, S. U. D. (1987). Adaptive Equalization, *In*: K. Feher, Ed. Advanced Digital Communications: Systems and Signal Processing Techniques, Prentice Hall Inc.

[12] Redfern, A. J., Zhou, G. T. (2001). A Root Method for Volterra System Equalization, *IEEE Signal Processing Letters*, 5 (11) 285-288.

[13] Redfern, A. J., Zhou, G. T. (2001). Blind Zero Forcing Equalization of Multichannel Nonlinear CDMA Systems, *IEEE Transactions on Signal Processing*, 49 (10) October. 2363-2371.

[14] Widrow, B., Stearns, S. D. (1985). Adaptive Signal Processing, Prentice-Hall, Inc., Englewood Cliffs, New Jersey.

[15] Hasan, Qadeer Ul ., Khan, Rafiqul Zaman., Levitin, Lev B.(2010). A Non-linear Adaptive Equalization Technique in Digital Satellite Communication, *GLOBUS: An International Journal of Management & IT*, 1 (2).